

## Note

# A Fast ICE Solution Procedure for Flows with Largely Invariant Compressibility

### INTRODUCTION

The ICE method of Harlow and Amsden [1] has proved a powerful one and has led the way to a whole series of variants with important practical applications. One such important class of applications deals with multidimensional transient two-phase (liquid-vapor) problems as they arise in safety evaluations of nuclear reactors subjected to certain postulated severe accident initiators [2, 3]. The basic approach is to couple continuity and momentum through an equation of state or an equation that governs the rate of phase change depending on the two-phase model assumed. Aside from the usual variations in differencing schemes and degrees of implicitness there are two basic approaches to achieving this coupling. The original one is based on the formulation and solution of a Poisson equation [1], by direct inversion or more commonly by iteration, for the pressure field. The other is based on direct iteration between momentum and continuity equations, the latter modified by use of a density-pressure relationship based on the equation of state or a phase changed law. Cell-by-cell or equation-by-equation iterations have been applied. In most recent applications the iteration approach has been preferred over that utilizing the Poisson equation on the basis of computational economy. However, for certain problems implementing the "proper" iteration procedures it is still more a matter of art rather than one of science and it may require substantial experience on the part of the user. Further, in applying the iteration approach some compromise must be made between accuracy and economy, and heuristic schemes, as, for example, addition of artificial viscosity and mass diffusion must be applied to compensate for the errors introduced due to "imperfect" convergence at each cycle. Both of these aspects can be crucial in achieving a stable and accurate solution in problems with large property gradients, such as for example in essentially incompressible flow fields (i.e., liquid-only) with embedded compressible region(s) (i.e., developing two-phase zones as in local boiling [3] or flashing).

The numerical scheme described here is based on the Poisson equation approach. However, the size of the linear system of equations to be solved at each computational cycle corresponds to the number of computational cells containing fluid whose compressibility varies substantially in comparison to that of the remaining essentially incompressible cells. For many problems this corresponds to substantial savings, (maximum benefit is achieved for flow fields with fully invariant

compressibility) and could be advantageously utilized even in comparison to iteration procedures. The additional advantage is that there is no accumulation of errors due to "imperfect" iteration convergence with beneficial stability and accuracy properties; hence good coupling between flow regions with greatly differing characteristics is obtained with a calculation that is not dependent upon artificial dampening for stability.

FORMULATION

In the final phase of the ICE method, when using cylindrical coordinates with axial symmetry, the system of equations becomes [1]

$$\begin{aligned} \bar{P}_{i,j} \left[ \frac{1}{c_{i,j}^n} + 2\theta\phi\delta t^2 \left( \frac{1}{\delta r^2} + \frac{1}{\delta z^2} \right) \right] \\ = G_{i,j} + \theta\phi\delta t^2 \left[ \frac{r_{i-1/2}\bar{P}_{i-1,j} + r_{i+1/2}\bar{P}_{i+1,j}}{r_i\delta r^2} + \frac{\bar{P}_{i,j-1} - \bar{P}_{i,j+1}}{\delta z^2} \right], \end{aligned} \quad (1)$$

where  $\bar{P}_{i,j}$  is the unknown "hybrid" pressure,  $\theta$  ( $0 < \theta < 1$ ) and  $\phi$  ( $0 < \phi < 1$ ) are weighting constants,  $G_{i,j}$  is a quantity which contains all available data for the  $n$ th time step, and  $c_{i,j}^n = (\partial p / \partial \rho)_{i,j}^n$  is related to the square of the sound speed. The above linear system of equations can be arranged in matrix form

$$\mathbf{A}\mathbf{X} = \mathbf{B}, \quad (2)$$

where  $\mathbf{A}$  is an  $M = i \times j$  banded matrix with the left side of Eq. (1) as its diagonal.  $\mathbf{B}$  is formed from  $G_{i,j}$  and the pressure boundary condition.

Upon investigation of the coefficient matrix  $\mathbf{A}$ , we found that provided  $\delta t$  is held constant, only the diagonal of  $\mathbf{A}$  varied in each computational cycle. Moreover, all terms on the diagonal are constant with time except for those that correspond to cells where the "sound speed" ( $c_{i,j}^n$ ) happens to differ from its initial value ( $c_{i,j}^0$ ). The matrix  $\mathbf{A}$  may be written as the sum of two matrices

$$\mathbf{A} = \mathbf{A}_0 + \mathbf{A}_1, \quad (3)$$

where  $\mathbf{A}_0$  consists of terms that remain constant (i.e., remain equal to their initial value) and  $\mathbf{A}_1$  is a diagonal matrix which contains only the variable terms. The terms of the  $\mathbf{A}_1$  matrix are represented by  $\epsilon_{k,k}$  where

$$\epsilon_{k,k} = \frac{1}{c_{i,j}^n} - \frac{1}{c_{i,j}^0} \quad (4)$$

and

$$k = i_{\max}(j - 1) + i.$$



Now since the  $A_1$  matrix contains two nonzero terms  $\epsilon_{kk}$  and  $\epsilon_{ll}$ , then the matrix product  $A_0^{-1}A_1$  will contain two nonzero columns, i.e.,

$$A_0^{-1}A_1 = \begin{bmatrix} 0 & \dots & a'_{1k}\epsilon_{kk} & \dots & 0 & \dots & a'_{1l}\epsilon_{ll} & \dots & 0 \\ 0 & \dots & a'_{2k}\epsilon_{kk} & \dots & 0 & \dots & a'_{2l}\epsilon_{ll} & \dots & 0 \\ \vdots & & \vdots & & \vdots & & \vdots & & \vdots \\ 0 & \dots & a'_{kk}\epsilon_{kk} & \dots & 0 & \dots & a'_{ll}\epsilon_{ll} & \dots & 0 \\ \vdots & & \vdots & & \vdots & & \vdots & & \vdots \\ 0 & \dots & a'_{n-1,k}\epsilon_{kk} & \dots & 0 & \dots & a'_{n-1,l}\epsilon_{ll} & \dots & 0 \\ 0 & \dots & a'_{nk}\epsilon_{kk} & \dots & 0 & \dots & a'_{nl}\epsilon_{ll} & \dots & 0 \end{bmatrix}. \quad (10)$$

We may define the matrix  $C$  and the vector  $D$  as

$$C = I + A_0^{-1}A_1 \quad (11)$$

and

$$D = A_0^{-1}B. \quad (12)$$

Equation (9) may thus be written as

$$CX = D \quad (13)$$

The elements of the matrix in Eq. (13) may be displayed as

$$\begin{bmatrix} 1 & \dots & a'_{1k}\epsilon_{kk} & \dots & 0 & \dots & a'_{1l}\epsilon_{ll} & \dots & 0 \\ 0 & \dots & a'_{2k}\epsilon_{kk} & \dots & 0 & \dots & a'_{2l}\epsilon_{ll} & \dots & 0 \\ \vdots & & \vdots & & \vdots & & \vdots & & \vdots \\ 0 & \dots & 1 + a'_{kk}\epsilon_{kk} & \dots & 0 & \dots & a'_{ll}\epsilon_{ll} & \dots & 0 \\ \vdots & & \vdots & & \vdots & & \vdots & & \vdots \\ 0 & \dots & a'_{n-1,k}\epsilon_{kk} & \dots & 0 & \dots & a'_{n-1,l}\epsilon_{ll} & \dots & 0 \\ 0 & \dots & a'_{nk}\epsilon_{kk} & \dots & 0 & \dots & a'_{nl}\epsilon_{ll} & \dots & 1 \end{bmatrix} \begin{bmatrix} X_1 \\ X_2 \\ \vdots \\ X_k \\ \vdots \\ X_l \\ \vdots \\ X_m \end{bmatrix} = \begin{bmatrix} d_1 \\ d_2 \\ \vdots \\ d_k \\ \vdots \\ d_l \\ \vdots \\ d_m \end{bmatrix}. \quad (14)$$

The diagonal elements of  $C$  are all one except in columns  $k$  and  $l$ . We may extract rows  $k$  and  $l$  from Eq. (14) and form a new system consisting of only two unknowns:

$$\begin{bmatrix} 1 + a'_{kk}\epsilon_{kk} & a'_{kl}\epsilon_{ll} \\ a'_{lk}\epsilon_{kk} & 1 + a'_{ll}\epsilon_{ll} \end{bmatrix} \begin{bmatrix} X_k \\ X_l \end{bmatrix} = \begin{bmatrix} d_k \\ d_l \end{bmatrix}. \quad (15)$$

Equation 15 may be solved by direct solution or if it is of large enough rank by iteration methods. Once this equation has been solved, the other terms in vector  $X$  may be solved for explicitly, for example,

$$X_p = d_p - a'_{pk} \epsilon_{kk} X_k - a'_{pl} \epsilon_{ll} X_l. \quad (16)$$

Thus in this example, the original ICE method required the solution of an  $m \times m$  linear system at each computational cycle while the new procedure requires the solution of an  $m \times m$  system only once *at the very beginning of the calculation* and the solution of a  $2 \times 2$  system at this particular computational cycle. On the other hand the limitations due to computer storage requirements for  $A_0^{-1}$  must be mentioned. Still 150-, 250-, and 500-cell computations are quite readily accessible with the CDC 6400, 7600, and IBM-195, respectively. It may be easily seen that changes of  $\delta t$  during the computation can also be accommodated by simply multiplying  $A_0^{-1}$  by  $\delta t_n^2 / \delta t_0^2$ , where  $\delta t_n$  is the time step utilized at the  $n$ th computational cycle and  $\delta t_0$  the time step for which the inverse  $A_0^{-1}$  has been calculated.

Naturally, if the number of highly compressible cells increases with time the rank of Eq. (15) approaches that of the full system Eq. (14) and the benefits diminish. However, for developing flows the integrated benefit can be still quite substantial. Since this approach is oriented to flow with Largely Invariant Compressibility, it will be referred to as ICE-LIC.

#### APPLICATION

The ICE-LIC method was incorporated into the HEV-2D computer code [5] which performs two-dimensional  $r = z$  boiling development calculations for a liquid sodium cooled rod-bundle (a fuel assembly for the Liquid Metal Cooled Fast Breeder Reactor-LMFBR), experiencing a severe power-to-flow mismatch transient. Such situations would correspond, for example, to accidental reactor power increase beyond rated levels, or to coolant flow coastdown (i.e., pump power loss) with failure of the reactor protection system to terminate the nuclear chain reaction (LOFA). The analysis of such events is extremely important in assessing the consequences of such accidents or providing mitigating factors as appropriate. Such analyses play an essential role in licensing the LMFBR, both in the U. S. and overseas [4, 5]. Due to neutronic feedback coolant boiling in current designs of commercial size LMFBRs leads to power increases. In a sense, therefore, coolant boiling drives the accident, and, its accurate numerical simulation, is essential to predicting the accident outcome. Further a most interesting aspect of this particular example chosen as application for ICE-LIC, is the possibility of boiling instabilities which may lead to rapid coolant expulsion from the flow channel. Such boiling instabilities are being calculated by current safety analysis codes [6] which model the coolant channel only in one (axial) dimension.

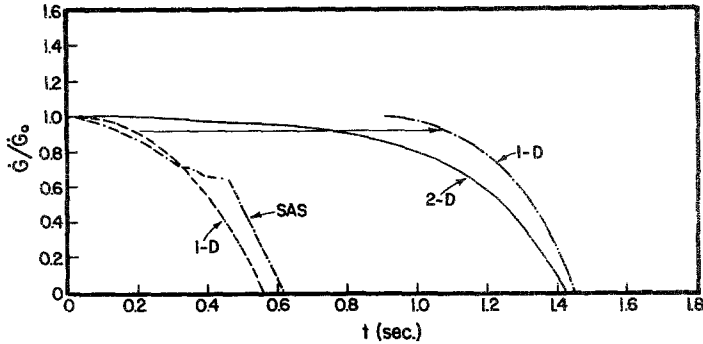


FIG. 1. Inlet flow transient comparisons between HEV-1D, HEV-2D and SAS [6] predictions. Zero time is taken at boiling inception.

In reality, however, the boiling develops in a two-dimensional fashion. The boiling zone will initiate at the hottest spot in the rod bundle, which is near the outlet and around the center of the channel that encloses the bundle of fuel rods. As the coolant continues to heat up this boiling zone will grow in all directions, and as it grows it will interfere (due to large volume of vapor production) with the liquid coolant flow as the coolant channel operates under prescribed pressure boundary conditions. This interference is that which leads to flow instability in the one-dimensional models and it is important to determine whether the real two-dimensional process is also susceptible to such flow instabilities.

A Loss-of-Flow Accident (LOFA) for the FFTF reactor is chosen for illustration here. The coolant channel is nearly 5 in. in diameter and its heated portion 36 in. long. At the time of boiling inception there is a 400° F temperature gradient across a radial distance near the top of the active core. For sufficient resolution, therefore, nearly five radial nodes are required. Similarly a very large number of axial nodes are required to meet resolution and accuracy requirements. This is a situation ideally suitable to ICE-LIC since early in the calculation only very few nodes will be compressible (boiling) and the remaining of this large flow field may be treated as nearly incompressible. As the boiling zone expands so will the size of the linear system that needs to be solved, however, only at the very end of the computation, when the whole flow channel is boiling, will the computational effort per cycle become comparable to that of the original ICE. In other words initially all  $\varepsilon$ 's are zero, at boiling inception one  $\varepsilon$  is nonzero and with time the number of nonzero  $\varepsilon$ 's increases. Noting the *nonlinear* effort increase with size for the solution of linear systems of equations the benefits in this case make the difference between achieving a "feasible" versus a "practical" solution. For the particular HEV-2D application reported here, 5000 time steps require 6 minutes of the CDC7600 for 128 computational cells (4 radial, and 32 axial). The equivalent one-dimensional, HEV-1D, version requires 2 sec for 2000 time steps and 31 (axial) nodes. For this particular application the  $\mathbf{A} \times \mathbf{A}_0^{-1}$  produced the unit matrix within  $10^{-12}$  in each element, and as a consequence conservation of mass and energy were observed with extremely tight accuracy.

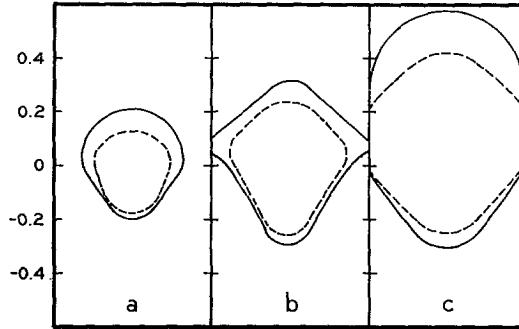


FIG. 2. Two-dimensional development of the boiling zone as flow reversal is approached. Axial position is normalized by the active core length. The zero position is at the top of the active core; (a) at 1.0 sec, (b) at 1.2 sec, and (c) at 1.4 sec following boiling inception.

The numerical results for this case indicate that the boiling zone quickly develops into a bubble-like, high in vapor content region, while the liquid coolant continues to flow and bypass this region in its periphery. This causes a dramatic reduction in the susceptibility of the flow to instabilities and results to a gradual boil-out instead of the rapid expulsion calculated for a one-dimensional model. This result is illustrated by the comparison of the inlet flow transient for the two models shown in Fig. 1. The good comparison of HEV-1D and SAS [6] results on the other hand indicate that the flow behavior is thermally controlled and it is quite independent of the particular two-phase flow model utilized. The bubble-like two-dimensional flow structure gradually becomes one-dimensional. Two vapor fraction contours, at three different times are given in Fig. 2. The inner contour represents nearly pure vapor ( $\sim 75\%$ ) while the outer contour marks the boiling inception boundary. The steep density gradient at the "bubble" boundary may be thus visualized. Following the transition to one dimensional behavior the transients calculated by HEV-1D and HEV-2D are in close agreement. In fact, Fig. 1 shows that the instability response yielding flow reversal in the HEV-1D results is identical, only delayed, in the 2D case by one second.

#### CONCLUSION

For the particular example of ICE-LIC application presented here the achieved computational stability and economy are crucial for high-resolution scoping or experiment-interpretation calculations but also for coupling more crude-noded versions to large system-wide accident analyses calculations.

#### ACKNOWLEDGMENTS

We would like to thank S. Gulik and R. Evans for incorporating the new procedure into the HEV-2D code. This work was supported by NRC Contract AT(40-24)-0181.

## REFERENCES

1. F. H. HARLOW AND A. A. AMSDEN, *J. Comput. Phys.* **8** (1971), 197.
2. C. W. HIRT AND T. A. OLIPHANT, "SOLA-PLOOP: A Nonequilibrium Drift-flux Code for Two-Phase Flow in Networks," LA-UR-76-1200, August 1976.
3. C. L. MIAO AND T. G. THEOFANOUS, in "Proceedings, Intl. Meeting on Fast Reactor Safety and Related Physics, Oct. 1976, Chicago, Illinois," USERDA CONF 761001, Vol. IV, pp. 1467-1476.
4. T. P. SPEIS, C. L. ALLEN, R. E. ALCOUFFE, R. P. DENISE, J. F. MEYER, W. E. KASTENBERG, AND T. G. THEOFANOUS. in "Proceedings, European Nuclear Conference, April 1975. Nuclear Energy Maturity," Vol. 5, pp. 774-801, Pergamon, New York, 1976.
5. T. G. THEOFANOUS, "Multiphase Transients with Coolant and Core Materials in LMFBR Core Disruptive Accident Energetics Evaluation." NUREG/CR-0224, 1978.
6. F. E. DUNN *et.al.*, "The SAS-2A LMFBR Accident-Analysis Computer Code." ANL-8138, Oct. 1974.

RECEIVED: October 29, 1976; REVISED: February 29, 1980

CHARLES C. MIAO AND T. G. THEOFANOUS,  
*School of Nuclear Engineering,*  
*Purdue University,*  
*West Lafayette, Indiana 47907*